AFRL-AFOSR-JP-TR-2019-0017

Shear induced solid-state joining of dissimilar titanium alloys

Rimma Lapovok
DEAKIN UNIVERSITY

07/15/2018
Final Report

Air Force Research Laboratory
AF Office Of Scientific Research (AFOSR)/ IOA
Arlington, Virginia 22203
Air Force Materiel Command

REPORT DOCUMENTATION PAGE

Form Approved
OMB No. 0704-0188

1. REPORT DATE *(DD-MM-YYYY)*	2. REPORT TYPE	3. DATES COVERED *(From - To)*
19-03-2019	Final	12 May 2016 to 11 May 2018

4. TITLE AND SUBTITLE
Shear induced solid-state joining of dissimilar titanium alloys

5a. CONTRACT NUMBER

5b. GRANT NUMBER
FA2386-16-1-4049

5c. PROGRAM ELEMENT NUMBER
61102F

6. AUTHOR(S)
Rimma Lapovok

5d. PROJECT NUMBER

5e. TASK NUMBER

5f. WORK UNIT NUMBER

7. PERFORMING ORGANIZATION NAME(S) AND ADDRESS(ES)
DEAKIN UNIVERSITY
221 BURWOOD HWY
BURWOOD, 3125 AU

8. PERFORMING ORGANIZATION REPORT NUMBER

9. SPONSORING/MONITORING AGENCY NAME(S) AND ADDRESS(ES)
AOARD
UNIT 45002
APO AP 96338-5002

10. SPONSOR/MONITOR'S ACRONYM(S)
AFRL/AFOSR IOA

11. SPONSOR/MONITOR'S REPORT NUMBER(S)
AFRL-AFOSR-JP-TR-2019-0017

12. DISTRIBUTION/AVAILABILITY STATEMENT
A DISTRIBUTION UNLIMITED: PB Public Release

13. SUPPLEMENTARY NOTES

14. ABSTRACT
Solid-state joining of dissimilar titanium alloys could be applied for many aerospace applications. Joining of dissimilar alloys during manufacturing, in particular asymmetric rolling (AR), is suggested for panel-to-panel construction. The role of shear strain during the solid-state joining of Ti-6Al-4V and Ti17 sheet materials by symmetric and asymmetric rolling was established. The mechanisms of interface-zone formation involved a combination of intermixing and inter-diffusion. Quantified by EDX analysis and TEM imaging, the interface-zone thickness was directly dependent on the level of shear strain. Post-joining tension and lap-shear measurements followed the same tendency, while annealing led to an opposite effect. For annealed samples, the decrease in interface-zone thickness with shear pre-strain and the concomitant loss of strength was rationalized on the basis of recovery and recrystallization during heat treatment and, therefore, the elimination of rapid-diffusion paths.
This work provided insight into the mechanisms of bond formation under conditions of large shear and high hydrostatic pressure. It shows that the concurrent asymmetric rolling of dissimilar titanium alloys with simultaneous nanostructuring of interface layer produced the high integrity bond and opens an avenue for production the bi-metalic titanium sheets with enhanced mechanical properties.

15. SUBJECT TERMS
Solid state joining, Dissimilar alloy, Titanium, Shear induced

16. SECURITY CLASSIFICATION OF:			17. LIMITATION OF ABSTRACT	18. NUMBER OF PAGES	19a. NAME OF RESPONSIBLE PERSON
a. REPORT	b. ABSTRACT	c. THIS PAGE			KNOPP, JEREMY
Unclassified	Unclassified	Unclassified	SAR		19b. TELEPHONE NUMBER *(Include area code)* 315-227-7006

Final Report for AOARD Grant FA2386-16-1-4049

"**Shear Induced Solid-State Joining of Dissimilar Titanium Alloys**"

Date

Name of Principal Investigators (PI and Co-PIs): Professor Rimma Lapovok

- e-mail address : r.lapovok@deakin.edu.au
- Institution : Institute for Frontier Materials, Deakin University
- Mailing Address : IFM, Deakin University, Geelong Waurn Ponds campus, Pigdons Road, Geelong Vic 3216, Australia
- Phone : +614 19897830
- Fax : NA

Period of Performance: May/12/2016 – May/12/2018

Abstract: Solid-state joining of dissimilar titanium alloys could be applied for many aerospace applications. Joining of dissimilar alloys during manufacturing, in particular asymmetric rolling (AR), is suggested for panel-to-panel construction. The role of shear strain during the solid-state joining of Ti-6Al-4V and Ti17 sheet materials by symmetric and asymmetric rolling was established. The mechanisms of interface-zone formation involved a combination of intermixing and inter-diffusion. Quantified by EDX analysis and TEM imaging, the interface-zone thickness was directly dependent on the level of shear strain. Post-joining tension and lap-shear measurements followed the same tendency, while annealing led to an opposite effect. For annealed samples, the decrease in interface-zone thickness with shear pre-strain and the concomitant loss of strength was rationalized on the basis of recovery and recrystallization during heat treatment and, therefore, the elimination of rapid-diffusion paths.

This work provided insight into the mechanisms of bond formation under conditions of large shear and high hydrostatic pressure. It shows that the concurrent asymmetric rolling of dissimilar titanium alloys with simultaneous nanostructuring of interface layer produced the high integrity bond and opens an avenue for production the bi-metalic titanium sheets with enhanced mechanical properties.

Introduction:

Solid-state joining (SSJ) of dissimilar titanium alloys is an attractive technology for many aerospace applications. In the past, SSJ by inertia-friction, linear-friction, and friction-stir welding [1, 2] has been shown to provide a number of benefits relative to arc welding due to short joining time, direct heat input at the weld interface, and a relatively-thin heat-affected zone [3]. Furthermore, friction-welding techniques are generally melt-free, enabling better control over grain size and structure, although the peak temperature at and near the weld interface can be very high and lead to the formation of brittle intermetallic compounds or other defects/porosity. For SSJ of Ti-6Al-4V and β21S, for example, the complex thermomechanical conditions in friction-stir welding have been observed to result in non-uniformity in the flow pattern, composition, and microstructure [4], all of which can be related to pin-rotation and translation effects. In other work [5], it was shown that rapid heating above the β-transus temperature and insufficient time at high temperature results in an inhomogeneous distribution of alloying elements and non-equilibrium microstructures in the weld zone [5]. The difference in mechanical and physical properties between the two joined materials can also result in the development of substantial residual stresses during cooling following the joining operation per se.

The focus of the present work was on the development of a SSJ process involving shear-induced inter-mixing and inter-diffusion at temperatures *below* the β-transus. In particular, the joining of sheet panels of dissimilar alloys via asymmetric rolling was investigated. This metal-forming operation induces severe shear as well as dilatational strains and thus enhances inter-mixing. The high strains also lead to nanostructuring of the material within the interface region and thereby accelerated

inter-diffusion [6]; i.e., the fine grain size increases the number of short-circuit paths for mass transport via grain-boundary diffusion and results in the formation of ultra-fast diffusion paths [7]. In addition, large shear strains promote the formation of vacancies, vacancy clusters, subgrain structures, and micro-shear bands. These features all contribute to an increase in both the bulk and grain-boundary diffusivities [8]. Therefore, asymmetric rolling of dissimilar titanium alloys might produce high-integrity bonds. The mechanical properties following joining could also be enhanced due to interfacial shear mixing and the formation of intermetallic compounds and/or unique microstructures within the interface zone. In the past, it has been demonstrated that high levels of nanostructuring cannot be achieved in single-phase alloys, however [9, 10]. The importance of high shear deformation was not recognized until recently, but it may crucial for the co-deformation and bonding of dissimilar alloys.
In the present work, the deformation and bonding of Ti-6Al-4V (Ti64) and Ti17 during symmetric rolling (SR) and asymmetric rolling (AR) were compared. This work provided insight into the mechanisms of bond formation under conditions of large shear and high hydrostatic pressure.

Aim of the project:

- To understand the enhancement of diffusion due to continuous formation of highly misoriented ultrafine grain structure
- To investigate the effect of shear on shear-induced bonding of two dissimilar titanium alloys and its role in simultaneous elimination of oxides from the surfaces.
- To establish a basic understanding of the effect of surface condition, such as surface roughness, on the quality of diffusion bonds.
- To study the fundamental mechanisms of formation nanostructured interface of two dissimilar titanium under severe shear deformation and high hydrostatic pressure

References:

[1] O. Roder, J. Albrecht, G. Lütjering, Microstructure and mechanical properties of an inertia friction welded INCOLOY alloy 909 – INCONEL alloy 718 joint for rotating applications, Materials at High Temperatures 23(3-4) (2006) 171-177.
[2] A.Y. Medvedev, V.M. Bychkov, A.S. Selivanov, S.P. Pavlinich, S.K. Dautov, A.V. Supov, Linear friction welding of two-phase titanium alloys VT6 and VT8-1, Welding International 29(1) (2015) 66-69.
[3] M. Esmaily, S. Nooshin Mortazavi, P. Todehfalah, M. Rashidi, Microstructural characterization and formation of α′ martensite phase in Ti–6Al–4V alloy butt joints produced by friction stir and gas tungsten arc welding processes, Materials & Design 47 (2013) 143-150.
[4] T.W. Morton, Solid State Joining of Dissimilar Titanium Alloys, PhD Dissertation, University of Washington, 2015, p. 225.
[5] A.L. Pilchak, T.F. Broderick, Evidence of a massive transformation in a Ti-6Al-4V solid-state Weld, JOM 65(5) (2013) 636-642.
[6] H.P. Ng, T. Przybilla, C. Schmidt, R. Lapovok, D. Orlov, H.-W. Höppel, M. Göken, Asymmetric accumulative roll bonding of aluminium–titanium composite sheets, Materials Science and Engineering: A 576 (2013) 306-315.
[7] S.V. Divinski, G. Wilde, Diffusion in ultrafine grained materials, Materials Science Forum 584-586 (2008) 1012-1017.
[8] S. Divinski, G. Wilde, E. Rabkin, Y. Estrin, Ultra-fast atomic transport in severely deformed materials—A pathway to applications, Advanced Engineering Materials 12 (2010) 779-785.
[9] R. Lapovok, H.P. Ng, D. Tomus, Y. Estrin, Bimetallic copper–aluminium tube by severe plastic deformation, Scripta Materialia 66 (2012) 1081-1084.
[10] A. Mendes, I. Timokhina, A. Molotnikov, P.D. Hodgson, R. Lapovok, Role of shear in interface formation of aluminium-steel multilayered composite sheets, Materials Science and Engineering A705 (2017) 142-152.

Experiment:

Materials

Ti64 and Ti17 sheets with dimensions 200 mm x 450 mm x 1.5 mm produced by Timet Division of PCC were used in this investigation. The final step in the process used by Timet was a heat treatment comprising 1110 K/4 h/water quench + 1140 K/4 h/water quench + 868 K/8 h/air cool. The nominal compositions of the two materials are summarized in Table 1. Preliminary rolling of the as-received materials to a 50% thickness reduction at RT and 500°C revealed a low ductility for Ti17; continuous cracks formed along the rolling direction for this alloy. Therefore, an additional annealing treatment (1023 K/4 h/water quench) was performed; this treatment enabled the successful rolling of Ti17 to a 50% reduction at 773 K.

The microstructures of Ti64 and Ti17 used in subsequent symmetric and asymmetric rolling (SR, AR) trials are shown in Fig. 1. In these scanning-electron-microscope (SEM), backscattered-electron (BSE) images, darker regions correspond to a low average atomic number (Z), and lighter regions to higher atomic number. The structure for Ti64 consisted of equiaxed, primary-α particles with an average size of ~10 μm within a transformed-β matrix of lamellar-alpha colonies (Fig. 1a). The Ti17 microstructure (Fig. 1b) comprised equiaxed, primary-α particles with a size of ~5 μm within the transformed-β-matrix of fine, lenticular-α platelets. In addition, some of the β grain boundaries were decorated with alpha phase.

Engineering stress-strain curves and mechanical properties for the two materials in the starting condition (Fig. 2, Table 1) indicated that Ti17 had slightly higher yield strength (YS) and ultimate tensile strength (UTS) compared to Ti64, while Ti64 was somewhat more ductile.

Table 1. Nominal compositions (wt. pct.) of the program alloys

Material	V	Al	Cr	Mo	Zr	Sn	Ti
Ti64	3.5 - 4.5	5.5 - 6.75					bal
Ti17		4.5 - 5.5	3.5 – 4.5	3.5 – 4.5	1.5 – 2.5	1.5 – 2.5	bal

Table 2. Mechanical properties of the program alloys in the starting condition

Material	YS (MPa)	UTS (MPa)	Total Elongation (Pct.)
Ti64	800	870	13
Ti17	865	990	9

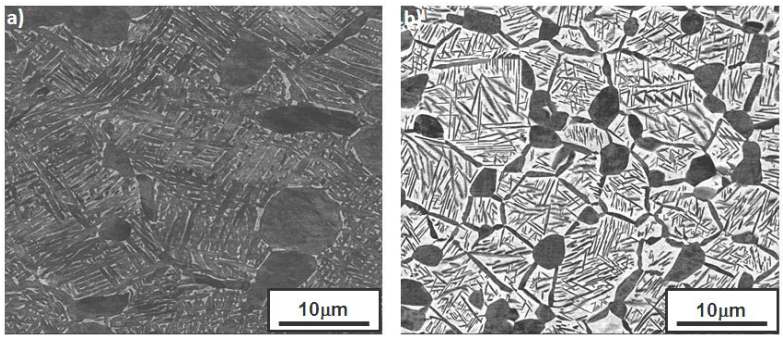

Fig. 1. BSE-SEM images of the microstructures of (a) Ti64 and (b) Ti17 before rolling.

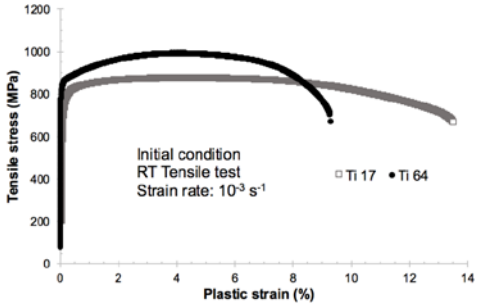

Fig. 2. Engineering stress-plastic strain curves for the starting conditions of Ti64 and Ti17.

Rolling trials

Samples of Ti64 and Ti17 having a width of 25 mm were pack rolled (without a can) using two different locations of the interface plane: (i) one coinciding with the central (mid) plane of the pack,

denoted as the “no-shift” condition, and (ii) one for which it was shifted toward the bottom roll, denoted as the “shift” condition. Rolling was performed using a two-high mill (manufactured by Carl Wezel Mühlacker) equipped with asymmetric rolls having a diameter ratio (d_r) of 1.0, 1.3, 1.6, or 2.0 [6]. In the present setup, the bottom roll had the larger diameter for asymmetric rolling with d_r > 1.The difference in roll size creates different rolling velocities on the top and bottom surfaces of the workpiece pack. Rolling with d_r = 2.0 resulted in severe cracking, however, and therefore all of the results reported below are for values of d_r between 1 and 1.6.

All rolling was performed at 773 K using an angular velocity of the rollers of 60 PRM, and total reduction of 50 pct. A muffle furnace with a protective argon atmosphere was used to preheat samples. For this purpose, each pack was soaked at the desired temperature for 10 min. and then rolled. After roll bonding, samples were water-quenched immediately to minimize microstructural changes.

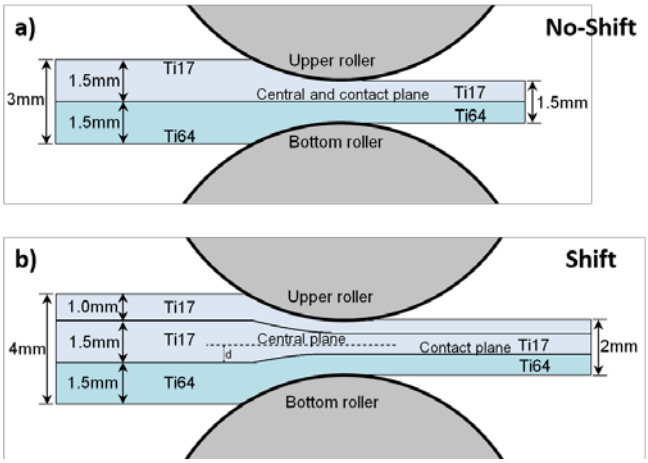

Fig. 3. Schematic illustrations of (a) rolling in which the contact plane coincided with the central (mid) plane of the pack and (b) rolling in which the contact plane was shifted toward the bottom roll.

The effect of surface preparation on bonding was also determined via symmetric rolling using packs having the contact plane coincident with the central plane, i.e., the no-shift condition. For this purpose, three different surface preparation techniques were applied: (i) grinding with 240 grit silicon-carbide (SiC) paper followed by wire brushing, (ii) sandblasting (grade C3 medium), and (iii) and fine grinding with 1200 grit SiC paper . After each surface treatment, the samples were cleaned with acetone to eliminate contaminants and grease from the contact surfaces. The surface roughness was measured using a Veeco WYKO NT1100 optical profilometer. The average roughness R_a was also determined based on at least 5 measurements at various locations over the sheet surfaces. Subsequently, the packs were assembled such that Ti64 was the bottom sheet, and the front edge was welded to prevent slippage during rolling.

Post-deformation annealing

Following each rolling experiment, the thermal stability of the microstructure was determined by excising selected samples and annealing under argon at 973 K for 4 h at in the muffle furnace.

Characterization techniques

The microstructures of the roll-bonded and annealed samples were determined by transmission electron microscopy (TEM) (using FEI Tecnai F20 and JEOL 2100F FEG TEMs) and SEM (using an FEI Quanta 3D FEG SEM). Both TEM and SEM analyses were made using longitudinal sections containing the normal direction (ND) and the rolling direction (RD). TEM foils were prepared from the interface joint via an in-situ focused-ion-beam (FIB) milling and lift-out technique in the FEI Quanta 3D SEM.

Lap-shear tests

Lap shear tests were performed to determine the strength of the bonds developed during rolling; Figure 4 shows a schematic of the test geometry. These tests were conducted at room temperature using an Instron 4505 universal testing machine equipped with a 100 kN load cell. Samples were loaded to failure at a displacement rate of 0.5 mm/min.

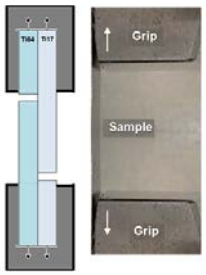

Fig. 4. Schematic illustration of a lap shear test

Tension tests

The mechanical properties of the processed sheets were established by uniaxial tension tests using an Instron 5500 universal testing machine equipped with a 30kN load cell. Tension samples with a reduced section dimensions 1.5-mm width x 10-mm length were cut parallel to the RD by electric discharge machining (EDM), and testing was conducted at room temperature using a constant crosshead speed corresponding to an initial strain rate of 1×10^{-3} s^{-1}.

The tension properties of monolithic sheets of Ti64 and Ti17, each rolled to a 50-pct. reduction via symmetric or asymmetric methods, were also determined and compared to those of the pack-rolled/bonded materials.

Results and Discussion:

Effect of rolling asymmetry d_r on microstructure evolution and joint formation

BSE-SEM observations revealed the effect of d_r on microstructure evolution and the nature of interface bonding in fine-ground, no-shift samples. A deformed $\alpha+\beta$ structure elongated along the RD was observed in both Ti64 and Ti17 for all processing trials (Fig. 5).The area fraction of primary α-particles in both materials is shown in Fig. 6. The results suggest it has not changed as a result of deformation and has not been contributed to by thick α-platelets. We also have not observed any obvious signs of particles fragmentation/spheroidization, which would confound the assessment of the structure. Therefore, we can use the thickness of the deformed primary α-particles as an indicator of the deformation imparted on the material. From Figure 5, it can be seen that an increase in d_r resulted in finer and more-elongated primary α-particles in regions adjacent to the interface in both materials. Measurements of the average thickness of the α-particles as a function of distance from the interface (Fig. 7) provided insight into rolling-induced strain heterogeneity. In the absence of particle fragmentation, the thickness for a *homogeneous* 50-pct. reduction would have been expected to be ~5 μm (= 0.5 x 10) for Ti64 and ~2.5 μm (=0.5 x 5) for Ti17. The results in Fig. 7 indicated that such was not the case, however.

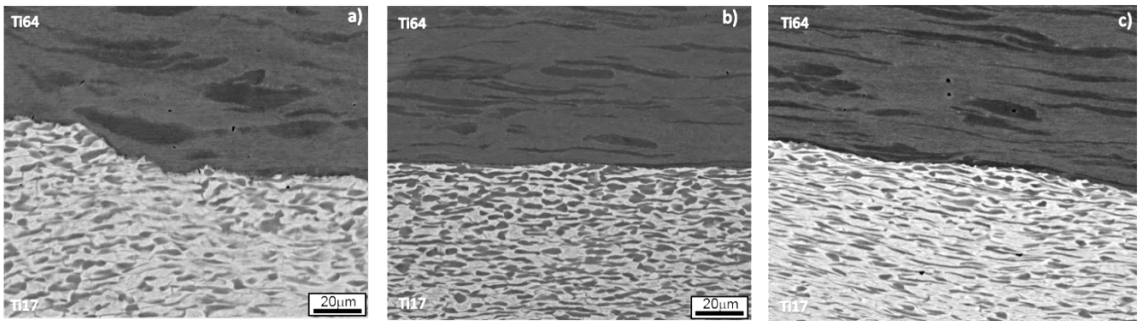

Fig. 5. BSE SEM images of the Ti64/Ti17 interface formed during rolling of samples with fine ground surfaces: (a) d_r = 1.0, (b) d_r = 1.3, and (c) d_r = 1.6.

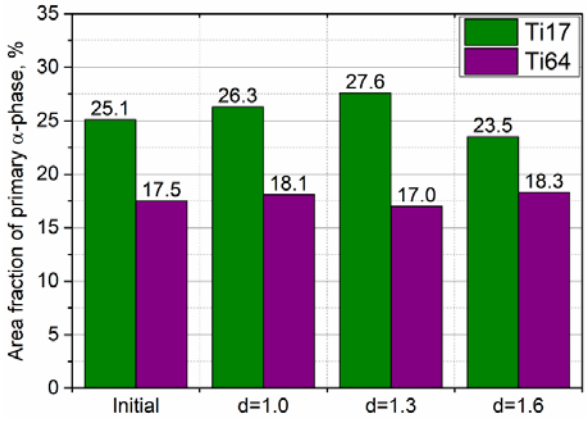

Figure 6. Area fraction of primary α-particles in Ti17 and Ti64 as a function of rolling asymmetry.

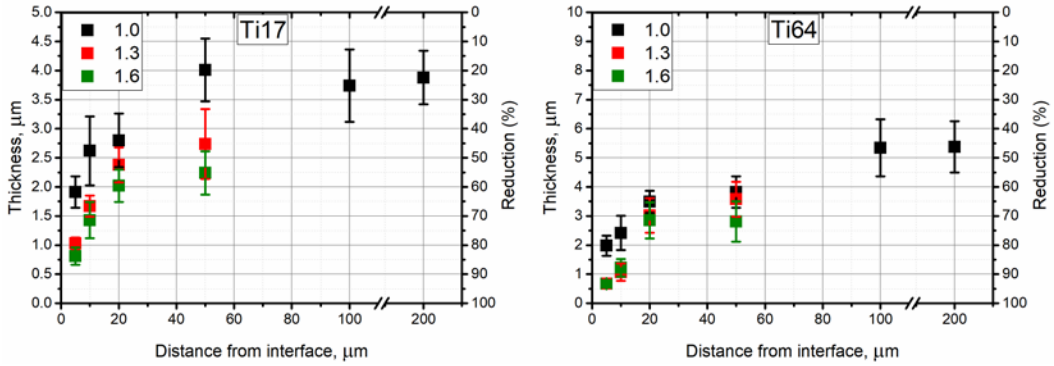

Fig. 7. Measurements from SEM BSE micrographs of the average α-particle thickness as a function of distance from the Ti64/Ti17 interface and rolling asymmetry (d_r).

From a quantitative standpoint, the data in Fig. 7 revealed that symmetric rolling (d_r = 1.0) led to a significantly greater thickness reduction of the α-particles in Ti64 (~50-80 pct.) compared with that for the α-particles in Ti17 (~20-60 pct.). Hence, it can be concluded that the majority of strain during rolling was imparted to the Ti64 layer. It is further confirmed via measurements at large distance from the interface, 100µm and 200µm, where the effects of the materials interactions is minimal. It is shown that the grain size for both materials reaches a plateau of around 50% reduction for Ti64 and 20-30% reduction for Ti17. This finding is not surprising in view of the lower strength and higher ductility of Ti64, albeit as determined at room temperature. Moreover, the particle thickness tended to increase with distance from the interface for both materials, thereby suggesting another factor contributing to the local deformation behavior. Despite the symmetry in the rolling process for these specific trials, it appears that plastic flow near the interface was influenced by friction, microscale slippage, and thus shear deformation on a micron/submicron scale. Indeed, the average initial roughness R_a of these samples was ~0.15 µm. It is therefore conceivable that the interaction of sheets with that level roughness could lead to additional local deformation to a depth of several microns from the interface.

A noticeable effect of asymmetry on differences in plastic flow of the two different materials was also observed (Fig.7). As evidenced by the strain gradient along the ND, asymmetric rolling introduced additional shear deformation due to the velocity difference between the top and bottom surfaces of the rolled packs. The results indicated that asymmetry gave rise to larger strain gradients in Ti17 than in Ti64. As a result, the difference in particle-size reduction (and hence strain) suffered by the two materials during symmetric rolling was noticeably diminished. It may be hypothesized that the reason for this behavior may lie with the inability of Ti64 to accommodate additional strain due to severe deformation (i.e., strain hardening) or texture hardening which would spread more deformation

into the Ti17 component of the pack. To investigate this possibility, finite-element-method (FEM) simulations of pack rolling were performed.

Bond-formation mechanism

TEM of regions at the interface of roll-bonded samples provided detailed insight into local microstructure evolution for pack geometries comprising either no shift (Figs. 8a,c,e) or shift (Figs. 8b,d,f).

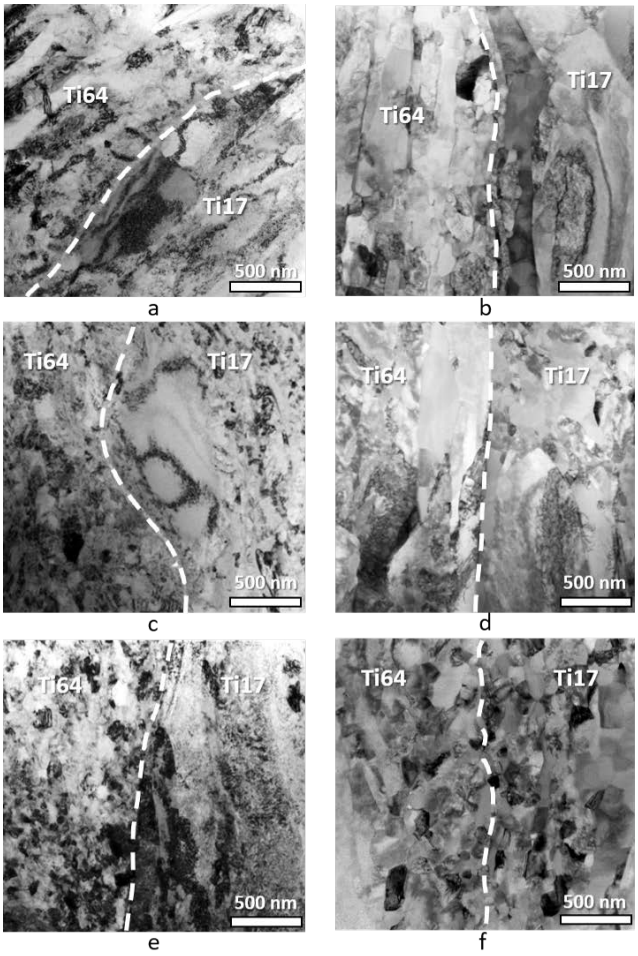

Fig. 8. Microstructure of the interface region in Ti64/Ti17 packs after rolling: (a) No-shift, d_r = 1.0, (b) shift, d_r = 1, (c) no-shift, d_r =1.3, (d) shift, d_r = 1.3, (e) no-shift, d_r = 1.6, and (f) shift, d_r = 1.6. The broken line indicates the position of the interface in each case.

For the symmetric, no-shift case (Fig. 8a), it was difficult to distinguish the α-particle sizes, although the substructures in the two materials were similar. In particular, it was noted that he average particle size in both materials at a distance of 5 μm from the interface was ~2μm, in line with the results reported in Fig. 7. An increase in asymmetry noticeably affected the substructure of Ti64; subgrains were gradually refined to a size of 100-150 nm. By contrast, changes in the structure of Ti17 were not as pronounced. While there were certain regions in Fig. 8b and c exhibiting elongated subgrains with a cross-section of ~100 nm (also shown in Fig. 9 and 10), there were still areas essentially devoid of subgrain boundaries, suggesting the effect of asymmetry was limited. This conclusion is somewhat contrary to the SEM findings, which indicated that the α-particle size of Ti17 was reduced with an increase in d_r. However, he scales of the SEM and TEM observations were vastly different in the two cases, and the mechanisms affecting micro- vs sub- structure evolution may be different. Furthermore, because of the localized nature of sliding and asperity interaction at the interface, there may also have been local temperature increases, which could confound interpretation of the deformation behavior.

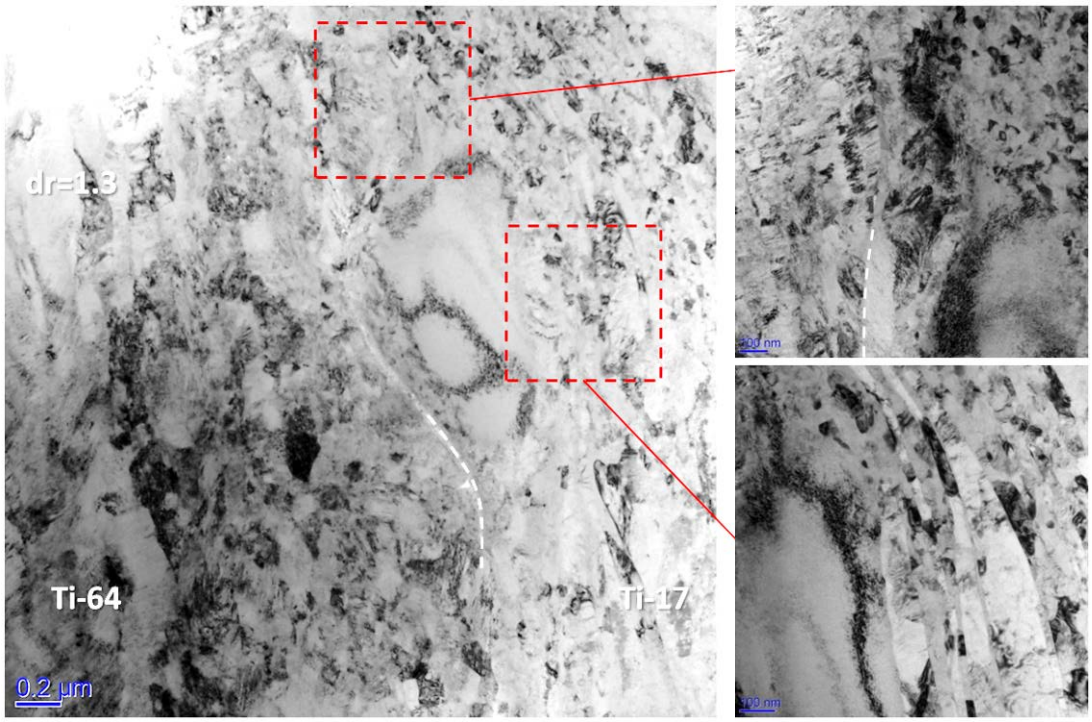

Fig. 9. Bright-field TEM micrographs of a sample processed with d_r = 1.3. The insets are higher magnification images for the highlighted areas. The broken line indicates the position of the interface in each case.

Additional TEM observations supported the above discussion regarding regions of fine, elongated subgrains in Ti17 (Fig. 9) and a definitive difference in the average subgrain size in the two materials after asymmetric rolling (d_r = 1.6), as evidenced by a comparison of the diffraction patterns for the two constituent materials (Fig. 12).

Figs. 8b,d,f shows the corresponding microstructures for pack geometries containing a shift in the interface location. The major difference between shift and no-shift samples was an apparent effect of additional shear on producing a more-uniform structure in both Ti64 and Ti17, regardless of rolling asymmetry. In particular, the microstructures of both alloys in Fig. 10f was very similar; they comprised uniaxial subgrains with a size of ~150-200 nm. Because of this similarity, it was difficult to discern the interface between the two alloys.

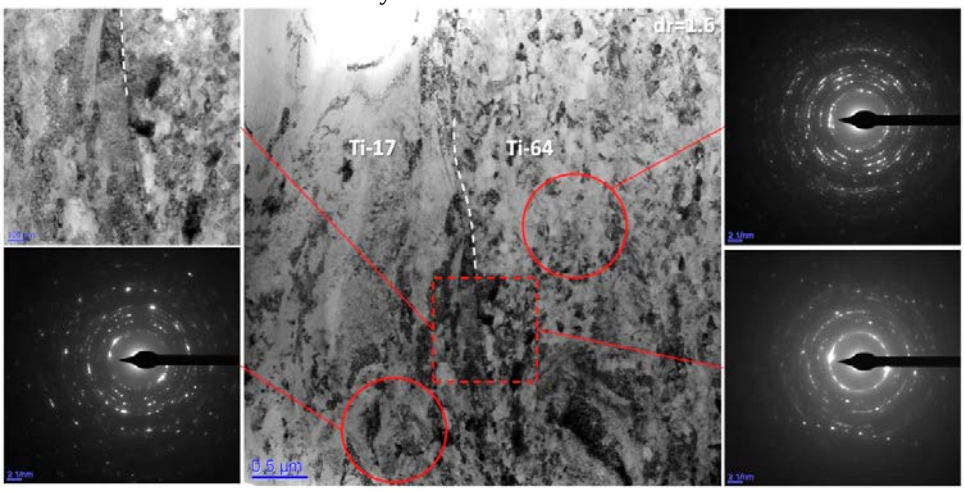

Fig. 10. Bright-field TEM micrographs of a sample processed with d_r = 1.6. The insets are higher magnification images for the highlighted areas. The broken lines indicate the position of the interface in each case.

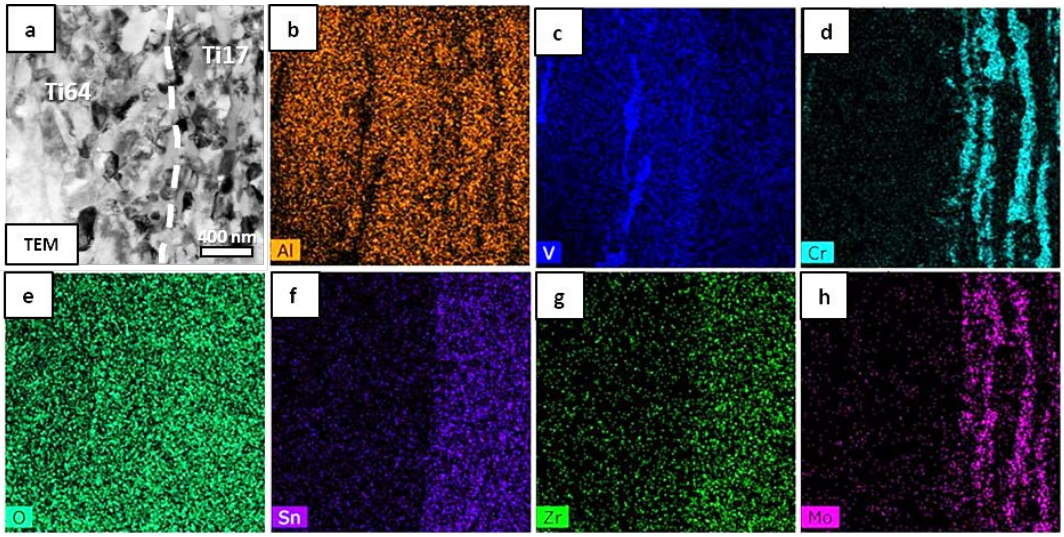

Fig. 11. EDX analysis of a shift sample processed using d_r = 1.6: (a) TEM of the region of interest, and (b-h) intensity of each element (except Ti) present in the two alloys.

EDX composition maps (e.g., Fig 11) readily indicated the bond interface for samples such as that in Fig. 10f. Identification of the interface based on vanadium content appeared to be the most beneficial because it is an important alloying element in Ti64, but is not used in Ti17. On the other hand, Cr, Mo, Zr and Sn are found only in Ti17. The first two of these elements are β-stabilizers and thus partition preferentially to the β-phase of this alloy, enabling differentiation of the β-phase (i.e., areas with high Cr and Mo contrast in Figs. 11d and h, respectively) from the α-phase in Ti17. Due to the limited amount of Cr and Mo in the α-phase in Ti17, however, defining the bond interface can be difficult if the alpha in Ti64 had come in contact with that in Ti17 at a specific location. The two other elements in Ti17, Sn and Zr, do not partition markedly between the two phases, and, hence, their concentration is almost uniform throughout the volume of Ti17 (Fig. 11f and g). Therefore, the interface location is most readily determined based on V in Ti64 and Cr and Mo in Ti17. As discussed below, these elements can also be used to assess the interface "thickness" and the degree of intermixing.

It should be noted that we also attempted to determine what phases came into contact in all of the cases studied. Since the only thing that can be reliably detected in the structure are β-phases, it was impossible to distinguish between primary and lamellar/acicular α-phase in the β-matrix. However, by circumstantial attributes, we could roughly estimate that in the majority of cases we observed the contact between the transformed matrices of the materials, similar to the case on Figure 13. Some of the cases indicated the contact between two primary α-particles, such as shown in Figure 15 below. The rest of the cases showed phase morphology that was too complicated, further compounded by severe grain distortion due to rolling and shear, rendering the difference between primary α-grains and transformed almost nonexistent.

Effect of post-deformation annealing on microstructure evolution in the interface zone

The effect of post-deformation annealing on the nature of the bond/interface-zone thickness was also assessed via microstructure and EDX analyses. A comparison of TEM images in Figures 8 and 12 showed that post-deformation annealing led to significant changes in substructure for all bonding conditions. Specifically, static recovery during annealing was clearly visible, as evidenced by the reduced density of defects and the lack of dislocation walls and bundles. Aspects of recrystallization were also noted, especially for shift samples after asymmetric rolling (Figs. 12d and 12f). These two conditions are also very interesting because they have both been shown to develop a relatively-uniform structure between the two materials during rolling (Figs 8d and 8f). Furthermore, a comparison of the substructures for shift and no-shift samples before annealing (Fig. 8) showed that the latter was more uniform with better-defined grain boundaries, while the subgrain structure was more pronounced in the former. Annealing thus may have led to a high level of recovery in the case of a pronounced subgrains structure, thereby eliminating small (low misorientation) subgrains and dislocation tangles, while it enhanced recrystallization and grain growth in the case of a better defined grain structure following rolling (e.g., Fig. 8f).

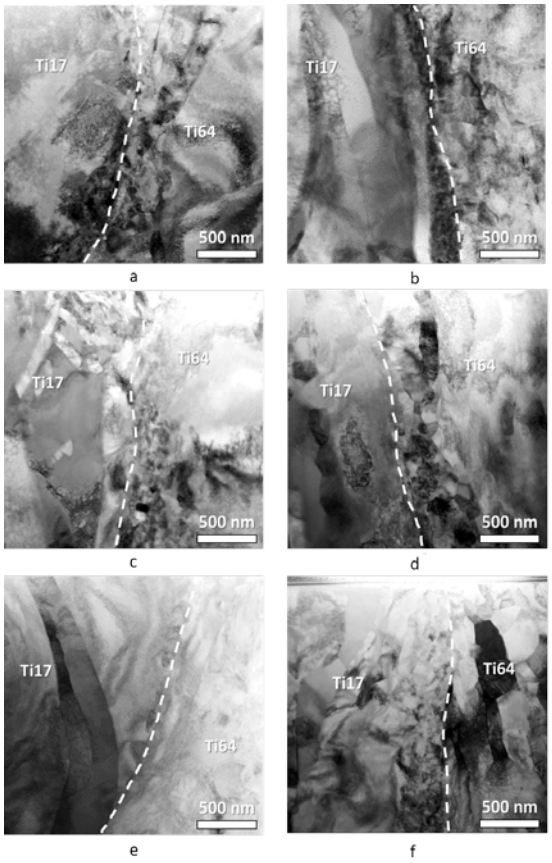

Figure 12. Microstructure at the interface region in Ti64/Ti17 samples after rolling and annealing: (a) No-shift, d_r = 1.0, (b) shift, d_r = 1.0, (c) no-shift, d_r = 1.3, (d) shift, d_r = 1.3, (e) no-shift, d_r = 1.6, and (f) shift, d_r = 1.6.

Although the interface was better defined for annealed samples, EDX helped to eliminate any remaining ambiguity with regard to the joint location. For the no-shift, d_r = 1.3 sample, for example, for which the interface location was complicated by the presence of several phases in Ti17 (Fig. 13), EDX analysis of the V, Zr, and Sn concentration profiles showed a clear indication of the boundary.

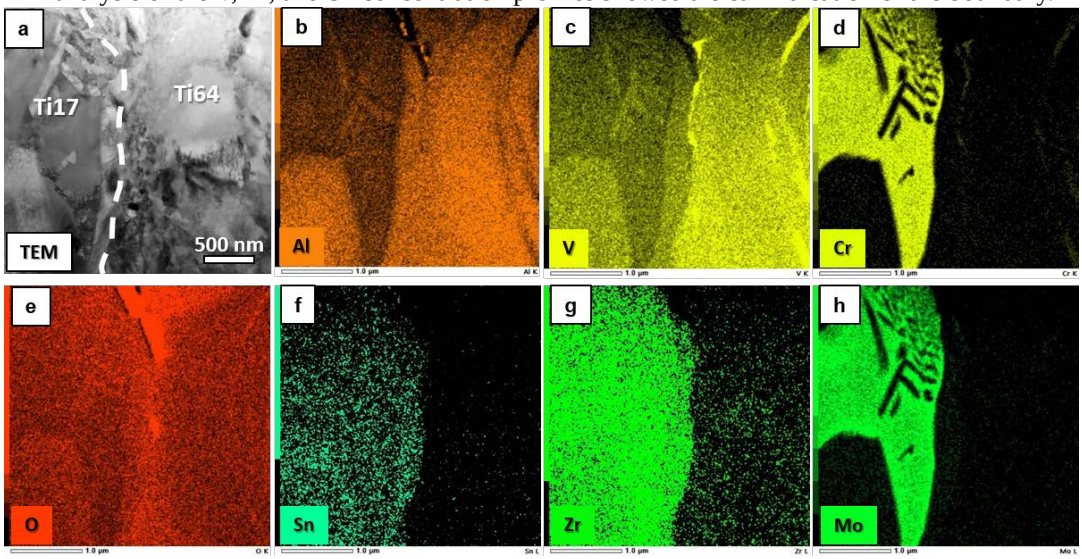

Figure 13. EDX analysis of a no-shift sample processed with d_r = 1.3 after annealing:
(a) TEM of the region of interest and (b-h) intensity of each of the elements
(b) (except Ti) present on both sides of the interface.

Effect of process parameters on inter-diffusion of alloying elements

EDX also provided quantitative insight into the gradients in concentration of various alloying elements in Ti64 and Ti17 and, thus, the estimates of the effective thickness of the inter-diffusion zone. Similar to the method used to establish the boundary location via EDX mapping, the concentrations of V and Sn (and, in some cases, Cr) were measured across the interface to determine the depth of inter-diffusion. The distance between points having the minimum concentration of each element was taken as the thickness of the inter-diffusion zone. Selected concentration profiles are shown in Fig. 14. The average values of the thickness of the inter-diffusion zone for all processing conditions are summarized in Table 3 and Fig. 15.

A number of trends were noted from these EDX measurements. In the as-rolled condition, there was an increase, albeit very small, in the thickness of the interface zone with the introduction of roll asymmetry and/or contact-plane shift (black symbols in Fig. 15). Overall, however, rather thin inter-diffusion zones were found, likely because of the low diffusivity associated with the low rolling temperature and the short processing time. Considering the limited resolution of the EDX, it is likely that in as-rolled samples, diffusion zone thickness was close to detection limit. It means that even if exchange of alloying elements has taken place, it is mostly due to physical intermixing rather than diffusion processes. Conversely, the entire difference between the thickness of the inter-diffusion zone in as-rolled and annealed samples should be a result of diffusion processes rather than intermixing, which is nonexistent when the sample is in a furnace.

In summary, it can be assumed that, for the most part, material transfer in as-rolled samples is due to mechanical intermixing of asperities, while in annealed samples is a result of diffusion across the boundary created via intermixing.

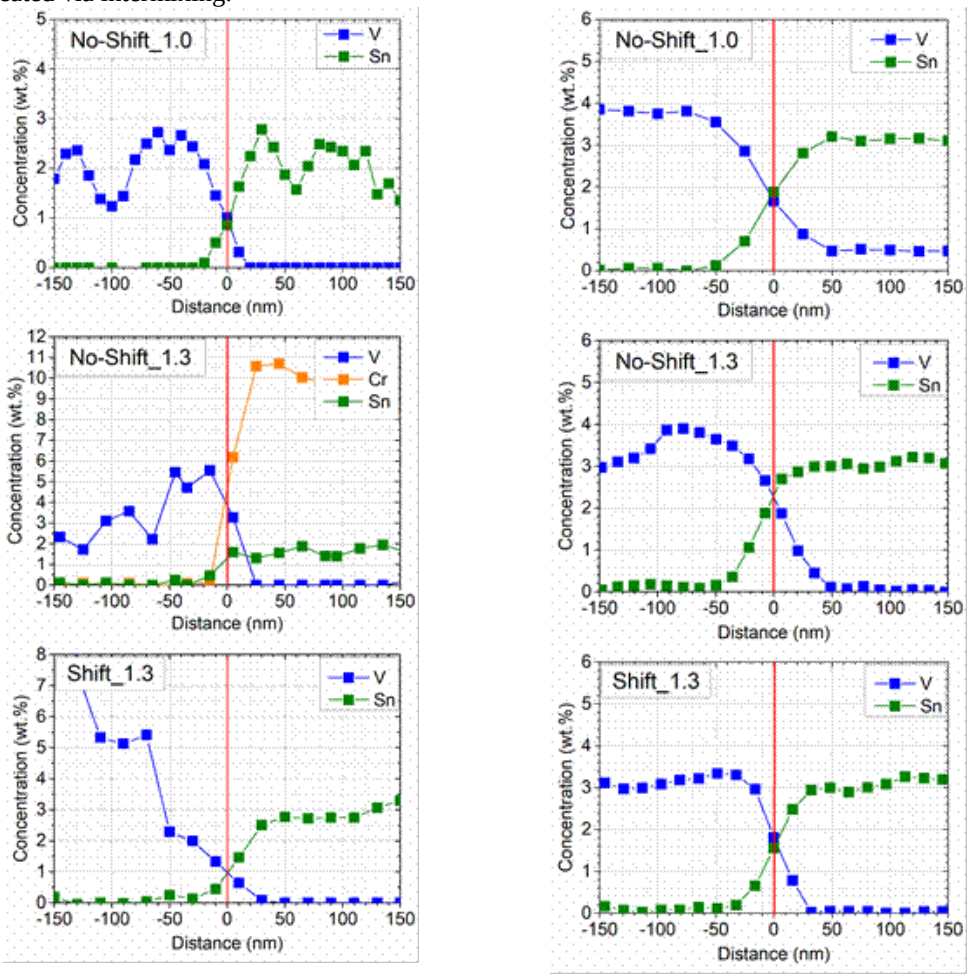

Figure 14. EDX line scans across the Ti64/Ti17 interface for selected shift and no-shift samples: (a) After rolling, or (b) after rolling and annealing.

Table 3. Thickness of the Ti64/Ti17 inter-diffusion zone in different conditions

Asymmetry, d_r	Thickness (nm)			
	No-Shift		Shift	
	As-Rolled	Annealed	As-Rolled	Annealed
1.0	39	97	48	145
1.3	42	82	52	123
1.6	51	64	61	87

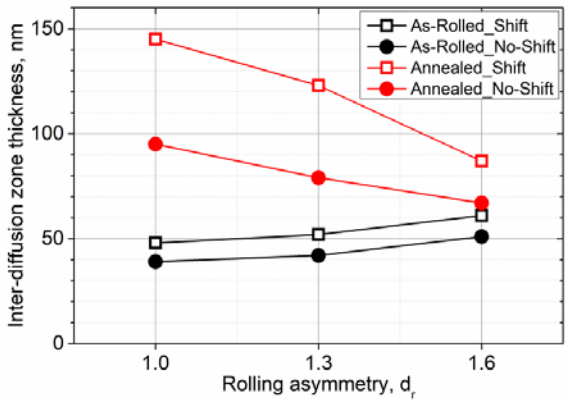

Figure 15. Inter-diffusion zone thickness of Ti64/Ti17 samples rolled using various process parameters.

On average, the thickness of the inter-diffusion zone increased during annealing 973 K, a temperature which was higher than that used for the rolling trials (773 K) (Fig. 15). Specific trends (Fig. 15) were more complex, however. It appeared that a shift in the interface plane yielded a thicker inter-diffusion zone, while roll asymmetry resulted in a reduction. This behavior can be rationalized by the fact that after rolling, static annealing results in recovery of the microstructure and partial recrystallization near the interface. From the analysis of the microstructure before and after annealing (Figs. 10 and 14), it was evident that recrystallization had taken place, thus increasing the grain size and removing high-diffusivity paths. Recrystallization started earlier in samples processed with a higher degree of shear, and therefore the diffusion was slowed more in these samples. Therefore, the thickness of the inter-diffusion zone was ultimately inversely proportional to level of shear strain introduced during rolling.

It is also important to note that the interface zone in the majority of the samples was composed primarily of α-phase in both of alloys. Because grain-boundary diffusion in α-Ti is almost three orders of magnitudes greater than bulk (volume) diffusion (pre-exponential values $D_{GB0} = 6.0\times10^{-7}$ and $D_{V0} = 8.6\times10^{-10}$ m^2/s, respectively, the α-particle/grain size, dislocation density, etc. in the two materials would have greatly influenced inter-diffusion.

Summary and Conclusions

The effect of roll asymmetry and the location of the interface (contact) plane on the solid-state joining of Ti-6Al-4V to Ti17 sheets was established. It was found that bond formation due to high, local shear strain and interface pressure results from a combination of mechanical intermixing and inter-diffusion. No evidence of the formation of intermetallic phases was observed. The thickness and strength of the bonded zone is proportional to the level of shear strain. The development of a nano-scale grain/subgrain structure at the interface likely enhances inter-diffusion.

Post-deformation annealing increases the thickness of the inter-diffusion zone, but is not beneficial for mechanical strength, which is reduced due to concomitant microstructural coarsening. Nevertheless, the present results do demonstrate that asymmetric rolling can be used to effect solid-state joining of dissimilar titanium.

List of Publications and Significant Collaborations that resulted from your AOARD supported project:

Manuscript: A. Mendes[1], A.E. Medvedev[1], R. Lapovok[1], S.L. Semiatin[2], Shear-induced, solid-state joining of dissimilar titanium alloys, ([1]Institute for Frontier Materials, Deakin University, Waurn Ponds, VIC 3216 Australia, [2]Air Force Research Laboratory, AFRL/RXCM, Wright-Paterson Air Force Base, OH 45433-7817, USA) is currently in preparation and will be submitted to 'Materials and Design' in July 2018)

f) Collaboration with Air Force Research Laboratory scientists – Dr Lee Semiatin

DD882: As a separate document, please complete and sign the inventions disclosure form.